Interactions between vacancies and prismatic Σ3 grain boundary in α-Al_2O_3: First principles study*

Fei Wang(王飞)[1,2], Wen-Sheng Lai(赖文生)[1,†], Ru-Song Li(李如松)[2], Bin He(何彬)[2], and Su-Fen Li(黎素芬)[2]

[1] *Laboratory of Advanced Materials, School of Materials Science and Engineering, Tsinghua University, Beijing* 100084, *China*
[2] *Xi'an High Technology Research Center, Xi'an* 710025, *China*

(Received 19 December 2015; revised manuscript received 19 January 2016; published online 20 April 2016)

Interactions between vacancies and Σ3 prismatic screw-rotation grain boundary in α-Al_2O_3 are investigated by the first principles projector-augmented wave method. It turns out that the vacancy formation energy decreases with reducing the distance between vacancy and grain boundary (GB) plane and reaches the minimum on the GB plane (at the atomic layer next to the GB) for an O (Al) vacancy. The O vacancy located on the GB plane can attract other vacancies nearby to form an O–O di-vacancy while the Al vacancy cannot. Moreover, the O–O di-vacancy can further attract other O vacancies to form a zigzag O vacancy chain on the GB plane, which may have an influence on the diffusion behavior of small atoms such as H and He along the GB plane of α-Al_2O_3.

Keywords: α-Al_2O_3, grain boundary (GB), vacancy interaction

PACS: 68.55.Ln, 68.35.–p, 68.90.+g **DOI:** 10.1088/1674-1056/25/6/066804

1. Introduction

Aluminum oxide, commonly referred to as alumina, is well known to have a broad technological significance. It is considered as a replacement gate oxide in the microelectronics industry, a substrate that is for growing the functional thin films, and as a support material for heterogeneous catalysts. Alumina has various allotropic forms of Al_2O_3, such as α-Al_2O_3, γ-Al_2O_3. Among the various allotropic forms, the stablest and well-characterized phase is α-Al_2O_3, which has a wide variety of technology applications such as high-temperature structure ceramics, dielectric insulators, and optical devices.

It was reported that the aluminum-rich coating with aluminum oxide is a very efficient hydrogen permeation barrier.[1–3] Moreover, both experimental and theoretical results showed that α-Al_2O_3 single crystal has a good resistance to hydrogen isotopic permeability.[4–6] Thus, α-Al_2O_3 has a potential application to the fusion reactor as a hydrogen isotopic permeation barrier in tritium production blankets to minimize tritium leakage. However, α-Al_2O_3 coatings, as a hydrogen isotopic permeation barrier, used in the engineering applications are often poly-crystalline. The presence of grain boundaries (GBs) and radiation-induced vacancies has a significant influence on the properties of α-Al_2O_3 coating against hydrogen isotopic permeation. It was reported that a rapid diffusion of oxygen along GBs via vacancies plays a crucial role in high temperature mechanical properties.[7–10] So far, it is still unclear whether there exists a rapid diffusion path along GBs via vacancies in α-Al_2O_3, which is crucial for the applications of α-Al_2O_3 coatings against hydrogen isotopic permeation. This motivates us to investigate the vacancy behavior near α-Al_2O_3 GBs.

Contrary to GBs, the formation energy of the point defect in perfect Al_2O_3 crystal has been systematically studied.[11–15] For instance, Xu *et al.*[16] studied the neutral and charged O vacancy in α-Al_2O_3 by supercell total-energy calculations using a first-principle method based on the density-functional theory. They obtained a theoretical zero-temperature O vacancy formation energy of 5.83 eV. However, the energetics of vacancies in α-Al_2O_3 GBs have not been well studied due to the fact that the atomistic structures of the GBs are complex. Recently, based on the fact that the atomic structure of pyramidal Σ13 twin GB has been characterized experimentally[17,18] and theoretically,[19] the defect energetics in pyramidal Σ13 twin GB of α-Al_2O_3 was investigated by Takahashi *et al.*[20] using a first principle projector-augmented wave method.

Apart from pyramidal Σ13 twin GB, the atomic structures of a few other GBs such as prismatic Σ3, basal Σ3, and rhombohedral Σ7 GBs have been characterized and proven to be periodic.[21–23] Among them, the prismatic Σ3 GB is special for its low GB energy and unique atomic layer structure, which consists of both Al and O atoms, in contrast to the other three GBs consisting of the atomic layers with either single Al or O atoms. From previous studies,[21] prismatic Σ3 GB has two possible structures: the screw-rotation twin and the glide-mirror twin. In the present study, we focus on

*Project supported by the National Key Basic Research and Technology Program, China (Grant No. 2010CB731601) and the National Natural Science Foundation of China (Grant No. 50871057).

†Corresponding author. E-mail: wslai@tsinghua.edu.cn

© 2016 Chinese Physical Society and IOP Publishing Ltd

the screw-rotation Σ3 twin GB with the lowest GB energy of 0.3 J/m^2 among the alumina boundaries studied so far by the first-principle. Moreover, the atomic arrangement of prismatic Σ3 GB has been investigated by density functional theory and transmission electron microscopy.[21] It is proven that this GB is quite periodic and thus suitable for constructing the supercell with the realistic number of atoms.

In this study, a first-principle projector augmented wave (PAW) method is used to study the mono-vacancies, di-vacancies and vacancy–clusters at or near prismatic screw-rotation Σ3 GB. Vacancy formation energies, vacancy–vacancy, and vacancy–cluster binding energies are calculated to reveal vacancy–GB interactions in α-Al_2O_3. The model and simulation details are described in Section 2, followed by the results and discussion in Section 3, and conclusion in Section 4.

2. Computational method and models

As shown in Fig. 1, the prismatic Σ3 $(10\bar{1}0)$ twin GB was obtained by rotating the right half of the α-Al_2O_3 crystal separated by the $(10\bar{1}0)$ plane with respect to the left half around $[10\bar{1}0]$ by 180° and then translating the right half crystal by a vector of $\frac{1}{2}\left[\bar{1}2\bar{1}0\right] + \frac{1}{3}[0001]$ parallel to the $(10\bar{1}0)$ plane. The GB was modeled using an orthorhombic supercell with cell dimensions along the x ($[\bar{1}2\bar{1}0]$), y ($[0001]$), and z ($[10\bar{1}0]$) directions of 4.80 Å, 13.11 Å, and 47.03 Å, respectively. In the model, only one GB plane lies between the left and right grains, and two $(10\bar{1}0)$ surfaces on other side of the grains were separated by a vacuum space of 15 Å in thickness to avoid their interactions when periodic conditions were applied to all three directions. There were 240 atoms (96 Al atoms and 144 O atoms) in the model. Since large supercells were used, numerical integrations over the Brillouin zone were performed at the Γ point.

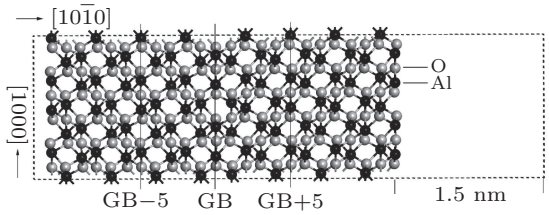


Fig. 1. Relaxed structure of S configuration of Σ3 $(10\bar{1}0)$ GB. The atoms are projected on the $(\bar{1}2\bar{1}0)$ plane. Black and gray balls represent Al and O atoms, respectively. The bold dark line indicates the GB and the light lines show the 5th atomic layers away from GB (noted by GB±5), which are selected as a reference for comparing the energy variation of vacancies at different atomic layers.

First principle calculations of prismatic Σ3 GB of α-Al_2O_3 were performed using a plane-wave-basis projector augmented wave(PAW) method[24] as implemented in the Vienna *ab initio* simulation package (VASP) code.[25–27] For the exchange correlation potential, the generalized gradient approximation (GGA)[28] was employed. In all the calculations, wave functions were expanded by plane waves with a maximum kinetic of 500 eV. The atoms, except for the outermost surface layers (fixed), were allowed to relax using a conjugate gradient scheme until their residual forces had converged to less than 0.01 eV/Å.

After optimizing the structure, we introduced a vacancy by removing an atom (Al or O) from different atomic layers away from GB and then calculated the vacancy formation energy. The GB system was treated neutrally without extra charges no matter whether vacancies were introduced. The vacancy formation energy is given by

$$E_{\rm f} = E_{\rm tot}({\rm vac}) - \{E_{\rm tot}({\rm perfect}) - n_{\rm Al}\mu_{\rm Al} - n_{\rm O}\mu_{\rm O}\}, \quad (1)$$

where $E_{\rm tot}$(vac) and $E_{\rm tot}$(perfect) are the total energies of the supercell with and without vacancies, respectively; $n_{\rm Al}$ and $n_{\rm O}$ are the numbers of Al and O atoms removed from the supercell; $\mu_{\rm Al}$ and $\mu_{\rm O}$ are chemical potentials of Al and O atoms in α-Al_2O_3, respectively. The $\mu_{\rm Al}$ and $\mu_{\rm O}$ are dependent on each other, they are constrained by the equilibrium conditions of

$$2\mu_{\rm Al} + 3\mu_{\rm O} = \mu_{\rm Al_2O_3}, \quad (2)$$

where $\mu_{\rm Al_2O_3}$ is a total energy per molecule of perfect α-Al_2O_3. Although $\mu_{\rm Al}$ and $\mu_{\rm O}$ are dependent on the conditions of growing α-Al_2O_3 crystal, the upper limits of $\mu_{\rm Al}$ and $\mu_{\rm O}$ are determined by the stability limit of α-Al_2O_3 in terms of total energies for metallic Al and molecule O_2 in the following manner

$$\mu_{\rm Al} \le \mu^0_{\rm Al}, \quad \mu_{\rm O} \le \mu^0_{\rm O}, \quad (3)$$

where $\mu^0_{\rm Al}$ and $\mu^0_{\rm O}$ are total energies per atom of Al metal and O_2 molecule, respectively. The formation enthalpy ($\Delta E_{\rm f}^{\rm Al_2O_3}$) of α-Al_2O_3 can be obtained from

$$\Delta E_{\rm f}^{\rm Al_2O_3} = 2\left(\mu_{\rm Al} - \mu^0_{\rm Al}\right) + 3\left(\mu_{\rm O} - \mu^0_{\rm O}\right). \quad (4)$$

From Eqs. (3) and (4), the range of $\mu_{\rm O}$ is represented as

$$\frac{1}{3}\Delta E_{\rm f}^{\rm Al_2O_3} + \mu^0_{\rm O} \le \mu_{\rm O} \le \mu^0_{\rm O}. \quad (5)$$

In order to obtain the range of $\mu_{\rm O}$, separate calculations of the total energies of fcc Al crystal and molecule O_2 were performed. The encut kept the same throughout all the calculations, i.e., 500 eV. For metallic fcc-Al, a $14 \times 14 \times 14$ Monkhorst–Pack mesh was used. In the case of oxygen, an isolated O_2 molecule was placed in a $1.5 \times 1.5 \times 1.5$-nm supercell, the calculation was performed with spin-polarized and $2 \times 2 \times 2k$-point meshes.

An O vacancy may attract another O vacancy to form an O–O di-vacancy. Their binding ability was described by binding energy, $E_{\rm b}(V_{O_1}V_{O_2})$, which is given by

$$E_{\rm b}(V_{O_1}V_{O_2}) = E_{\rm f}(V_{O_1}) + E_{\rm f}(V_{O_2}) - E_{\rm f}(V_{O_1}V_{O_2}), \quad (6)$$

where $E_{\rm f}(V_{O_1})$ and $E_{\rm f}(V_{O_1}V_{O_2})$ are the formation energies of a single O_1 vacancy and O_1–O_2 di-vacancy, respectively .

Similarly, the binding energy, $E_b(V_{Al})$, of an Al vacancy to a vacancy cluster $V_{nO}V_{(m-1)}$ Al that contains n O vacancies and $m-1$ Al vacancies, is determined as follows:

$$E_b(V_{Al}) = E_f(V_{nO}V_{(m-1)Al}) + E_f(V_{Al}) - E_f(V_{nO}V_{mAl}), \quad (7)$$

where $E_f(V_{Al})$ and $E_f(V_{nO}V_{mAl})$ are the formation energies of a single Al vacancy and the vacancy cluster V_{nO} V_{mAl} with n O vacancies and m Al vacancies, respectively.

3. Results and discussion

3.1. Mono-vacancy

An O/Al vacancy is introduced by removing an O/Al atom from the relaxed structure as shown in Fig. 1. The calculated formation energy, E_f, of vacancies lying on the GB plane is given in Fig. 2. It can be seen that the E_f of V_O increases with increasing μ_O and *vice versa* for V_{Al}. There is a small difference among E_f values at different sites on the GB plane due to their different coordination numbers. The calculated formation energies for Al and O vacancies agree well with the results of previous studies (e.g. the maximum value for V_{Al} (V_O) is 12.46 (6.51) eV compared with 12.21 (6.42 eV),[29] respectively.)

As a general tendency, it is often assumed that the E_f of vacancies near to the GB is smaller than those in the bulk-like region. As shown in Fig. 1, the 5th atomic layer on the right side away from the GB (denoted as GB+5) is treated as a bulk-like region and taken as a reference for the consideration of variation of E_f with vacancy site. The differences in E_f among different atomic layers with respect to the reference (hereafter called ΔE_f) are calculated and shown in Fig. 3. It can be seen that ΔE_f reduces zigzag with reducing the vacancy distance to the GB for V_O, while it monotonically decreases and then bounced on the GB plane for V_{Al}. One notices that the minimum E_f for V_O occurs on the GB plane and that for V_{Al} appears at the 1st atomic layer away from the GB. Interestingly, it can be seen that the minimum ΔE_f for V_{Al} almost triples that for V_O. The minimum E_f for V_{Al} is not located on the GB but 1st atomic layer is away from the GB, because the structural distortion for vacancy sites on the GB is bigger than that on 1st atomic layer away from the GB.[11] A negative value of ΔE_f indicates that vacancies are more preferably formed at the GBs rather than in bulk. By scrutinizing Figs. 2 and 3, one may draw a conclusion that O vacancies are more readily formed and aggregate to the GB than Al vacancies in α-Al_2O_3 because the E_f of O vacancies is generally smaller than that of Al vacancies.

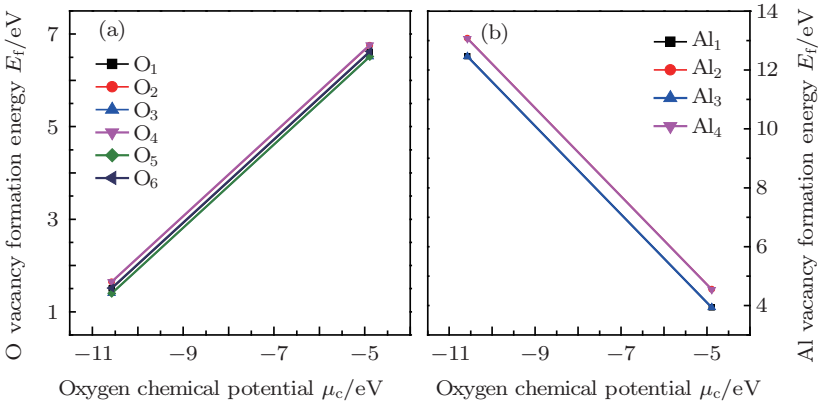


Fig. 2. (color online) Variations of the calculated formation energy of (a) neutral oxygen vacancy V_O and (b) neutral aluminum vacancy V_{Al} at various sites on the prismatic Σ3 S GB plane of α-Al_2O_3 with oxygen chemical potential μ_O. The different atomic sites on the GB plane are indicated by the different numbers.

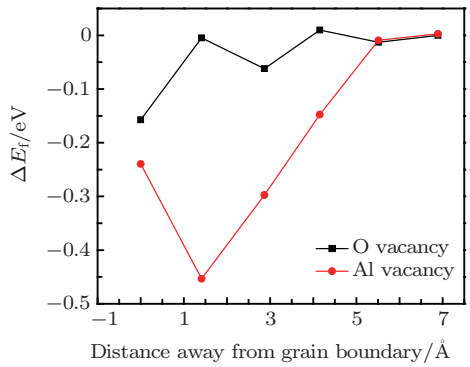


Fig. 3. (color online) Variations of system energy with vacancy site away from the GB plane. ΔE_f is the difference in energy between the vacancy at different atomic layers and that at the reference state (i.e., the 5th atomic layer away from the GB).

3.2. Di-vacancy

As is well known, di-vacancy configurations play an important role in vacancy aggregation into a large vacancy cluster in oxides. As discussed above, a mono-vacancy tends to migrate to GB areas, it is of interest to know whether a mono-vacancy located at the GB area would attract other vacancies to form a cluster in GB areas. One vacancy is chosen and fixed at the site with the lowest formation energy and another vacancy is varied and selected at different atomic layers. Figure 4 shows the difference in the system energy, ΔE, as a function of distance between two vacancy sites (i.e., $\Delta E = E_{tot}(r) - E_{tot}(\text{ref})$, where $E_{tot}(r)$ is the system energy

with two vacancies separated by r and $E_{\rm tot}$(ref) is the system energy with one vacancy fixed at the minimum $E_{\rm f}$ site and another at GB+5). It can be seen that the system energy decreases with reducing the distance between two vacancies for both O–O and O–Al (or Al–O) di-vacancy, and vice versa for Al–Al divancancy. It indicates that the O vacancy on the GB plane attracts another nearby O vacancy while the Al vacancy repels other Al vacancies to close the O vacancy. It can also be seen that the binding energy $E_{\rm b}$ reaches a maximum when the O–O and O–Al (or Al–O) di-vacancy are the first nearest neighbor at the GB, and it is remarkably large for the Al–O di-vacancy as compared with that for the O–O di-vacancy. We find that both in bulk alumina, the binding energies for the Al–O di-vacancy are also much larger than those for the other two di-vacancies. The large binding energies of unlike species of vacancies have also been observed in other oxides, such as Y_2O_3.[30]

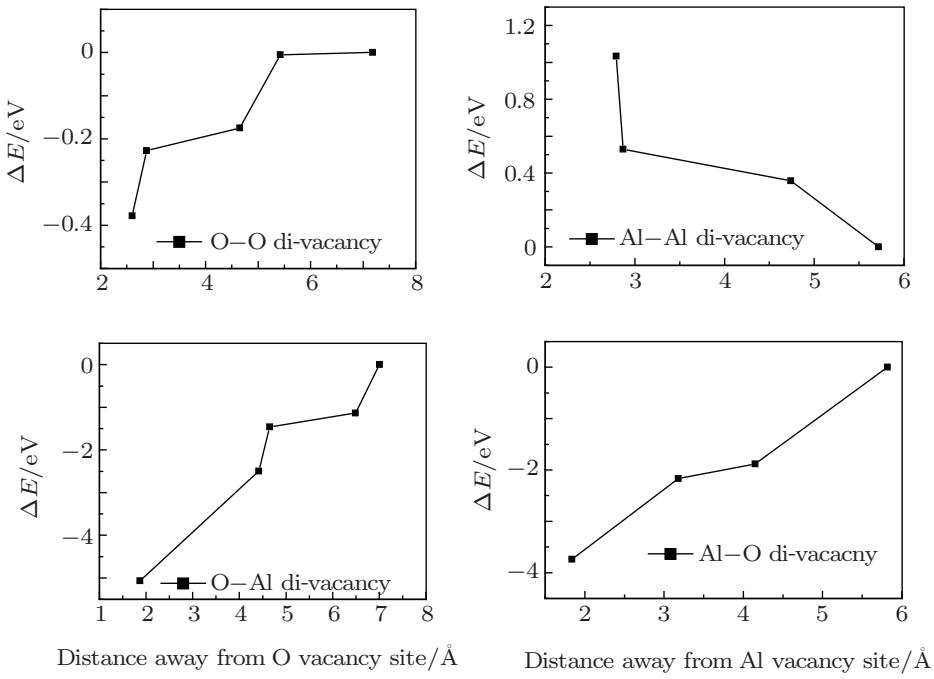


Fig. 4. Variations of the difference of system energy, ΔE, with distance between two vacancy sites.

3.3. O-vacancies chain

In the stoichiometric α-Al_2O_3, the concentration of O atoms is 1.5 times that of Al atoms. Moreover, as can be seen in Fig. 2, the formation energy of the O vacancy is in general lower than that of the Al vacancy. Therefore, in the radiation environments the radiation-induced O vacancies will be much more than Al vacancies. As mentioned above, the binding energy of the Al–O di-vacancy is remarkably larger than that of the O–O di-vacancy. In addition, we find that the binding energy of the Al–O di-vacancy keeps almost unchanged no matter whether they are located in the bulk or at the GB. Therefore, in the radiation environments the radiation-induced Al vacancies can easily attract the O vacancies to form Al–O di-vacancies, which are difficult to move once they have formed. This will prevent Al vacancies from aggregating to the GB. However, for O vacancies, because the number of O vacancies at the GB is large and their formation energy is small, they tend to aggregate to GBs. As the binding energy of the O–O di-vacancy is larger in GB areas than in bulk, an O vacancy at the GB can attract other O vacancies nearby to form an O–O di-vacancy. It is wondered whether the O–O di-vacancy could further attract other O vacancies to GBs to form an O cluster.

The O-vacancy chains consisting of O vacancies on or near the GB plane are the most possible form for vacancy clusters near the GB as shown in Fig. 5(a). The binding energy, $E_{\rm b}$(O), of an extra O vacancy to the existing vacancy chain with $(n-1)$ O vacancies is calculated as a function of O vacancy number n, and the results are given in Fig. 6. It can be seen that $E_{\rm b}$(O) is always positive for the O vacancy chain marked by number 1 on the GB plane, while it turns negative when the numbers of vacancies n reaches 3 and 4 for the chains labeled by number 2 and 3, respectively. The negative binding energy represents the repulsion between an extra O vacancy and the existing O vacancy chains to hinder the growth of O vacancy cluster. However, all the O vacancies on the GB plane could bind together to form a zigzag O vacancy chain as shown in Fig. 5(b). It can be deduced that if such a vacancy chain exists, it would play an important role in diffusion of small atoms such as H, He through the GB plane. Therefore, it would have a significant influence on the behavior of α-Al_2O_3 against tritium permeation, which is worth further study.

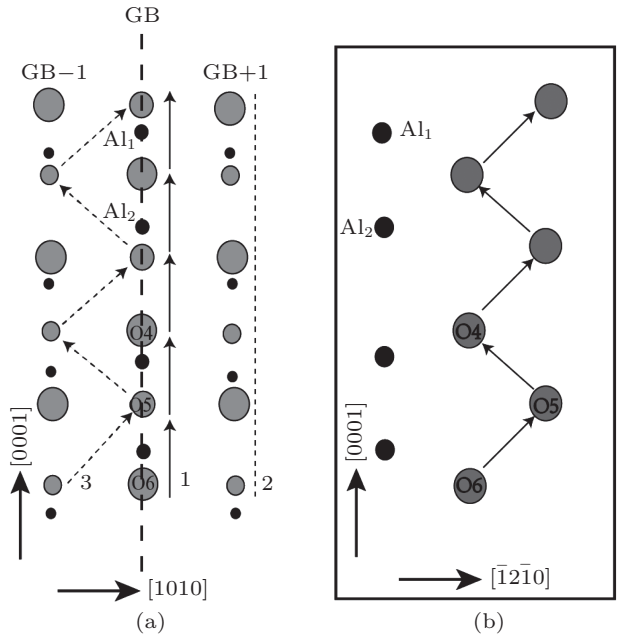


Fig. 5. (a) Three possible configurations of O-vacancy chains in the GB areas. The O-vacancy chain on the GB plane (GB+1) marked by the number 1 (2) is indicated by the solid line with arrays (dashed line) and the zigzag chain between GB-1 and GB planes marked by the number 3 is shown by the dashed lines with arrays. (b) The side view of the zigzag O vacancy chain denoted by the number 1 on the GB plane.

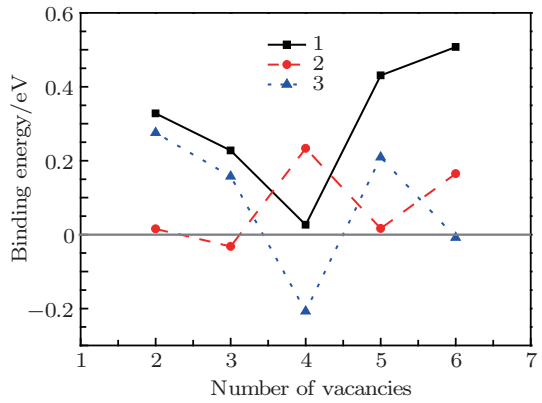


Fig. 6. (color online) Plots of the binding energy E_b(O) of an extra O vacancy to the vacancy chain with $(n-1)$ O vacancies versus the number of vacancies for the three possible O-vacancy chains as shown in Fig. 5.

4. Conclusions

A first principles calculation is performed to study the interactions between vacancies and prismatic Σ3 screw-rotation grain boundary in α-Al_2O_3. It turns out that the lowest vacancy formation energy for O (Al) vacancy occurs on the GB plane (the atomic layer next to the GB), suggesting that monovacancy tends to aggregate to GB areas. The O vacancies located on GB areas can attract other O vacancies nearby to form an O–O di-vacancy while Al vacancy cannot. The O–O divacancy can further attract other O vacancies to form a zigzag O vacancy chain on the GB plane, which is energetically favorable.

References

[1] Aiello A, Ciampichetti A and Benamati G 2004 *J. Nucl. Mater.* **329** 1398
[2] Li L, Sang G, Zhang P C and Jiang G 2007 *Acta Phys. Chim. Sin.* **23** 1912
[3] Zhang G K, Wang X L, Xiong Y F, Shi Y, Song J F and Luo D L 2013 *Int. J. Hydrogen Energ.* **38** 1157
[4] Hollenberg G W, Simonen E P, Kalinin G and Terlain A 1995 *Fusion Engineering and Design* **28** 190
[5] Forcey K S, Ross D K and Wu C H 1991 *J. Nucl. Mater.* **182** 36
[6] Belonoshko A B, Rosengren A, Dong Q, Hultquist G and Leygraf 2004 *Phy. Rev. B* **69** 024302
[7] Cannon R M, Rhodes W H and Heuer A H 1980 *J. Am. Ceram. Soc.* **63** 46
[8] Heuer A H, Tighe N J and Cannon R M 1980 *J. Am. Ceram. Soc.* **63** 53
[9] Lagerlof K P D, Mitchell T E and Heuer A H 1989 *J. Am. Ceram. Soc.* **72** 2159
[10] Heuer A H and Lagerlof K P D 1999 *Philos. Mag. Lett.* **79** 619
[11] Dienes G J, Welch D O, Fisher C R, Hatcher R D, Lazareth O and Samberg M 1975 *Phys. Rev. B* **11** 3060
[12] Catlow C R A, James R, Mackrodt W C and Stewart R F 1982 *Phys. Rev. B* **25** 1006
[13] Grimes R W 1994 *J. Am. Ceram. Soc.* **77** 378
[14] Lagerlof K P D and Grimes R W 1998 *Acta Mater.* **46** 5689
[15] Matsunaga K, Tanaka T, Yamamoto T and Ikuhara Y 2003 *Phys. Rev. B* **68** 085110.
[16] Xu Y N, Gu Z Q, Zhong X Fu and Ching WY 1997 *Phys. Rev. B* **56** 7277
[17] Hoche T and Ruhle M 1996 *J. Am. Ceram. Soc.* **79** 1961
[18] Hoche T, Kenway P R, Kleebe H J, Finnis M W and Ruhle M 1994 *J. Phys. Chem. Solids* **55** 1067
[19] Nakamura K, Mizoguchi T, Shibata N, Matsunaga K, Yamamoto T and Ikuhara Y 2007 *Phys. Rev. B* **75** 184109
[20] Takahashi N, Mizoguchi T, Tetsuya T 2009 *Mater. Trans.* **50** 1019
[21] Fabris S, Nufer S, Elsasser C and Gemming T 2002 *Phys. Rev. B* **66** 155415
[22] Marinopoulos A G, Nufer S and Elsasser C 2001 *Phys. Rev. B* **63** 165112
[23] Chen F R, Chu C C, Wang J Y and Chang L 1995 *Phi. Mag. A* **72** 529
[24] Blochl P E 1994 *Phys. Rev. B* **50** 17953.
[25] Kresse G and Hafner J 1993 *Phys. Rev. B* **47** 558
[26] Kresse G and Furthmuller J 1996 *Comput. Mater. Sci.* **6** 15
[27] Kresse G and Furthmuller J 1996 *Phys. Rev. B* **54** 11169
[28] Perdew J P, Burke K and Ernzerhof M 1996 *Phys. Rev. Lett.* **77** 3865
[29] Lei Y K, Yong Y, Duan Z Y and Wang G F 2013 *Phys. Rev. B* **87** 214105
[30] Ou Y D and Lai W S 2011 *Nucl. Instrum. Method Phys. Res. B* **269** 1720